Reactivity of Alkaline Lignite Fly Ashes Towards CO 2 in Water

ARTICLE *in* ENVIRONMENTAL SCIENCE AND TECHNOLOGY · JUNE 2008

Impact Factor: 5.33 · DOI: 10.1021/es702760v · Source: PubMed

Environ. Sci. Technol. **2008,** *42,* 4520–4526

Reactivity of Alkaline Lignite Fly Ashes Towards CO_2 in Water

MARTIN BACK,* MICHAEL KUEHN, HELGE STANJEK, AND STEFAN PEIFFER

Department of Hydrology, University of Bayreuth, BayCEER, D-95440 Bayreuth, Germany, Applied Geophysics, RWTH Aachen University, D-52065 Aachen, Germany, and Clay and Interface Mineralogy, RWTH Aachen University, D-52065 Aachen, Germany

Received November 2, 2007. Revised manuscript received March 18, 2008. Accepted March 26, 2008.

The reaction kinetics between alkaline lignite fly ashes and CO_2 ($pCO_2 = 0.01-0.03$ MPa) were studied in a laboratory CO_2 flow-through reactor at 25–75 °C. The reaction is characterized by three phases that can be separated according to the predominating buffering systems and the rates of CO_2 uptake. Phase I (pH > 12, < 30 min) is characterized by the dissolution of lime, the onset of calcite precipitation and a maximum uptake, the rate of which seems to be limited by dissolution of CO_2. Phase II (pH < 10.5, 10–60 min) is dominated by the carbonation reaction. CO_2 uptake in phase III (pH < 8.3) is controlled by the dissolution of periclase (MgO) leading to the formation of dissolved magnesium-bicarbonate. Phase I could be significantly extended by increasing the solid–liquid ratios and temperature, respectively. At 75 °C the rate of calcite precipitation was doubled leading to the neutralization of approximately 0.23 kg CO_2 per kg fly ash within 4.5 h, which corresponds to nearly 90% of the total acid neutralizing capacity.

Introduction

Among the various CO_2 sequestration scenarios, mineral trapping is regarded to be the most promising technique with regard to a permanent and inherently safe storage of CO_2 (*1*). Carbonation of Ca- and Mg-rich minerals (e.g., wollastonite) is well-known from natural weathering processes (*2*) and may have the capacity to bind the global CO_2 emission from fossil fuel combustion (*1*). Since the carbonation process proceeds with slow reaction kinetics (*2*), its acceleration by technical means has been widely studied (*3, 4*). However, the use of natural silicate minerals is generally associated with high energy and economic costs, and it is therefore discussed critically (*5*).

Alternatively, alkaline ashes from combustion processes are proposed as a feedstock material that is cheap, highly reactive and that is generated as a byproduct of power generation (*6–8*). In this work, we present results from an experimental study on the reaction between fly ashes from lignite combustion and CO_2 in aqueous solution. Lignite fly ashes are available in large amounts in many coal combusting countries and commonly have a high acid neutralizing capacity (ANC) of up to 7 meq g^{-1} (*9*). In Germany, about 15 million tons of lignite fly ashes accumulate per year that are being mainly deposited in landfills (*9*). Hitherto, studies on the reactivity of fly ashes had been performed mainly with respect to the long-term leaching behavior (*10–12*) classifying them as nonhazardous waste material (*13*). Our knowledge about the short-term reactivity of fly ashes with CO_2 is, however, scarce.

In particular, we aim to establish a general model for the mechanisms controlling the CO_2 transfer to the ash minerals at a time scale relevant for a technical solution. We have, therefore, set up experiments to study CO_2 storage by lignite fly ashes in aqueous suspensions at low temperature (25–75 °C) and CO_2 partial pressures comparable to flue gas observed from lignite combustion (0.01–0.03 MPa). These conditions allow to mimic CO_2 removal from flue gas at a distinctly lower energy demand compared to other CO_2 sequestration techniques (*5*). The aqueous route was chosen because generally higher reaction rates are observed compared to the gas–solid route (*14*). The effect of transport phenomena at the solid–liquid and gaseous–liquid interfaces on the rate of CO_2 transfer was tested by variation of the stirring rate in the suspensions. Similarly, the effect of solution chemistry on mineral dissolution and CO_2 transfer mechanisms was studied by variation of the solid–liquid (s/l) ratios.

Experimental Section

Sample Characterization. Fly ashes from a lignite coal power plant (Neurath, Germany) were used in this study. The fly ashes were collected from the first filtering step of connected electrostatic precipitators and stored in containers sealed from ambient air. Residual coal particles >250 μm were separated from the ashes by sieving.

The chemical composition of the fly ashes was determined using X-ray fluorescence analysis (XRF) after measuring and correcting for the loss of ignition (LOI) at 1150 °C. The mineralogical composition was studied by X-ray powder diffraction (XRD) with a Huber 423 goniometer with scans run from 2° to 110° (2θ, Co Kα), increments of 0.018° and 10 s counting time per step. Quantitative phase analysis based on the Rietveld technique was performed with the program BGMN (*15*). Due to the common problem of mineral phase quantification in materials containing amorphous phases we added an internal standard (ZnO) which enabled to recalculate the proportion of unaccounted phases during the Rietveld procedure. The single-point BET surface area of the fresh fly ashes was determined by using a porosimetry system (Micromeritics ASAP 2010). Particle size distribution was measured by laser diffraction (Malvern Mastersizer 2000) after decomposition of organic matter with H_2O_2 (30%) and dispersion of the suspension in an ultrasonic bath. SEM pictures were taken using a LEO-1450VP SEM equipped with an EDX system (Inca, Oxford Instruments).

Experiments

A 3.7 L batch reactor facility (ALF, Bioengineering) was used to perform experiments in the presence of CO_2 at different solid–liquid ratios, partial pressure of CO_2 (pCO_2), stirring rates, and temperatures. Control experiments in the absence of CO_2 were run in a nitrogen atmosphere. The experimental setup is shown under Supporting Information section A.

The ashes were inserted through a port at the top of the reactor using a funnel. The electrical conductivity (EC), pH, pCO_2, and temperature were recorded continuously during each experimental run. The suspension was sampled periodically and filtrated (nylon filter: 0.45 μm) to analyze the composition of both the solid and the liquid phase. Solid samples were freeze-dried and homogenized to determine the mineralogical (XRD) and elemental composition (XRF).

* Corresponding author phone: +49-921-55-2170; fax: +49-921-55-2366; e-mail: martin.back@uni-bayreuth.de.

10.1021/es702760v CCC: $40.75
Published on Web 05/20/2008

TABLE 1. Relative Mineralogical Composition of the Lignite Fly Ash before and after 10 Minutes of CO_2 Treatment (s/l-ratio: 75g L^{-1}, pCO_2: 0.02 MPa, stirring rate: 450 rpm, *T*: 25 °C)

mineral phase (Rietveld analysis)	wt.-% unreacted	wt.-% CO_2-treated after 10 min
brownmillerite	20.5	20.5
anhydrite	13	7
lime	11.5	3
periclase	11.5	11.5
Na_2SO_4	5	0
calcite	3.5	6
quartz	3	3
amorph. compounds	28.5	42.5
ettringite	0	3.5

The content of organic carbon was determined as the difference between the total carbon content (as measured with an element analyzer) of unreacted samples and samples after dissolution in HCl. The filtrate was acidified with 1 vol.-% of HNO_3 (65%). Main (Ca, Mg, Na, K, S) and trace elements (Al, Ba, B, Cd, Mn, Fe, and Sr) were determined by ICP-OES.

The suspension was flushed with CO_2 at different partial pressures (10−30% at atmospheric total gas pressure) that were obtained after mixing of N_2 and CO_2 at different proportions with two mass flow controllers (MKS Instruments, type 258C) at a total gas flow of 1 L min^{-1}. The gas was bubbled into the solution through a gas frit.

The CO_2 uptake of the system (mmol g^{-1}) was determined by measurement of the CO_2 concentration of the exhaust gas using an optical IR-sensor (Vaisala, GMP221) and from known gas fluxes. The partial pressure of CO_2 was calculated from the CO_2 concentration measured at atmospheric gas pressures:

$$\text{CO}_2 \text{ uptake (mmol g}^{-1}) = \sum_i^n \frac{(\text{pCO}_{2\text{in}} - \text{pCO}_{2\text{out}})_i \cdot \Delta t \cdot Q}{R \cdot T \cdot M} \quad (1)$$

pCO_{2out}: mean value of pCO_2 in the outflow in a 10 s time (Δt) interval (10^{-3} N m^{-2}). *Q* is the flow rate (m^3 s^{-1}), *R* is the gas constant (0.083144 atm L mol^{-1} K^{-1}), *T* is the temperature (K), and *M* is the mass of fly ash (g).

The IR sensor had a response time T_{63} (cf. Supporting Information section B) of 20 s which implies a certain delay upon fast changes of the measured pCO_2. The water temperature was kept constant and equilibrated with a certain pCO_2 before the addition of the ashes into the reactor. The stirring rate was varied between 150−600 rounds per minute, rpm and the s/l-ratio between 25−100 g L^{-1}.

Total dissolved inorganic carbon (TDIC) was determined as CO_2 in a gas sample taken from gastight vials after acidification of a sample taken from the reactor with a gastight syringe. After filtering the sample through a nylon filter (0.45 μm), 0.5−1 mL of the solution was injected into N_2 purged vials containing 100 μL of HCl ($c = 6$ mol L^{-1}). CO_2 was measured by gas chromatography with a TCD/FID detector. The amount of TDIC was calculated applying Henry's law considering the known volumes of headspace and solution:

$$\text{TDIC} = \frac{\text{ppm}}{10^6}\left(K_H + \frac{V_G}{R \cdot T \cdot V_W}\right) \quad (2)$$

V_G is the gas volume of headspace (L), V_W is the volume of solution (L), and K_H is the henry constant ($10^{-1.41}$ mol L^{-1} atm^{-1} at 25 °C).

The mass transfer of CO_2 into solid metal−carbonate was calculated as the difference between the total uptake of CO_2 and TDIC. The accuracy of this method was tested as described under Supporting Information section B. Ca conversion was calculated from the amount of precipitated calcite and the amount of Ca in solution normalized to the Ca content of the initial fly ash.

The reactor system was equipped with an automatic titration system, which allowed to perform pH-stat experiments in a N_2 atmosphere to determine the ANC of the fly ashes and the release of the main elements at pH 7−10 (c(HCl) = 1 mol L^{-1}). Additionally, pH-stat experiments were run with NaOH ($c = 1$ mol L^{-1}) in deionized water to measure the specific dissolution rate of CO_2 at varying pH (*7–10*) and stirring rates (300−700 rpm). The effect of the variable ionic strength was not considered in these experiments.

Results and Discussion

Composition of Fly Ashes. Combined XRD/Rietveld analysis (Table 1) of the untreated ashes revealed the occurrence of brownmillerite ($Ca_2(Fe_{1.634},Al_{0.366})_2O_5$), anhydrite ($CaSO_4$), periclase (MgO), lime (CaO), calcite ($CaCO_3$), sodium sulfate (Na_2SO_4), quartz (SiO_2) and traces of gehlenite ($Ca_2Al_2SiO_7$), magnetite (Fe_3O_4), portlandite ($Ca(OH)_2$), and microcline ($KAlSi_3O_8$), respectively. The content of noncrystalline phases was calculated to be 28.5 wt.-% which seem to be mainly molten glass as indicated by the SEM images (cf. Supporting Information section D). The main elements in terms of wt-%. of oxides were CaO (37.3 ± 3), MgO (15.4 ± 0.4), SO_3 (13.7 ± 0.7), Fe_2O_3 (10.1 ± 1), SiO_2 (8.7 ± 2.5), Na_2O (3.4 ± 0.4),

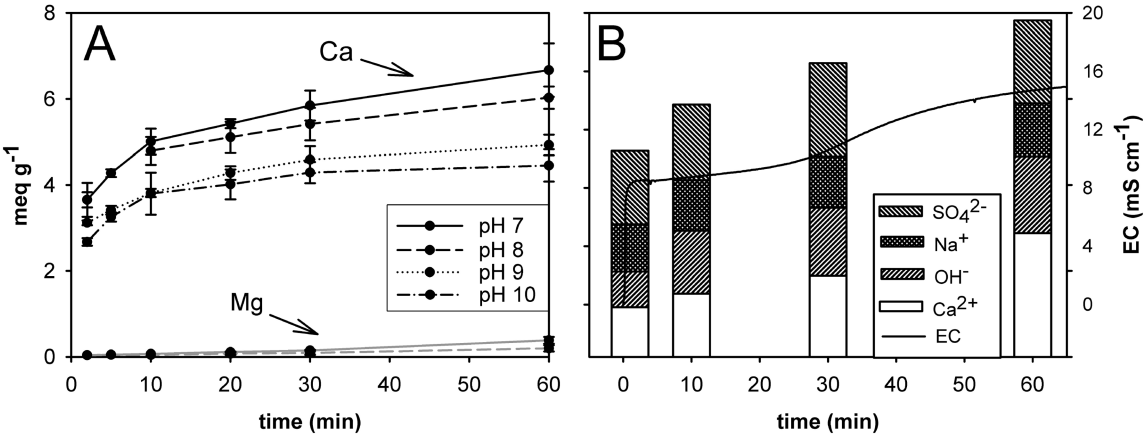

FIGURE 1. Batch experiments with deionized water and fly ash at a s/l-ratio of 12.5 g L^{-1} and a temperature of 25 °C under nitrogen atmosphere. A: Release of Ca and Mg (meq g^{-1}) during pH-stat-experiments. B: Release of main elements (meq g^{-1}). The pH was always > 12.

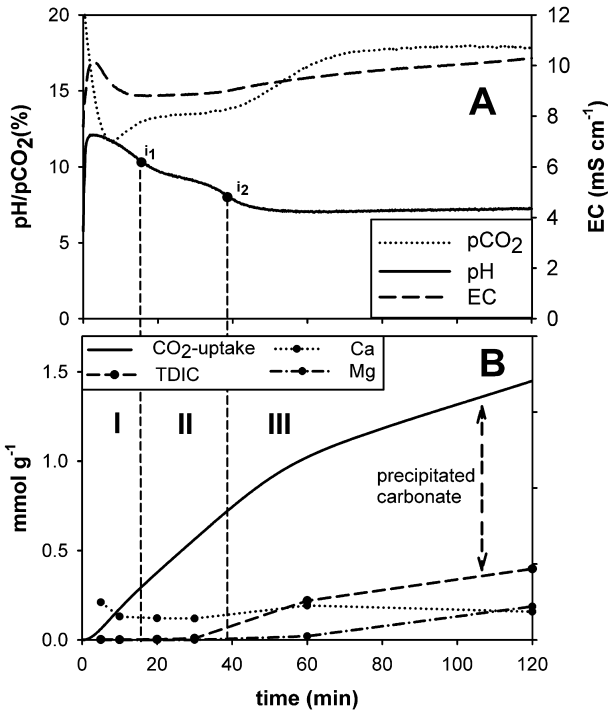

FIGURE 2. Reaction progress in fly ash experiment with water and CO_2 (s/l-ratio = 75 g L^{-1}; initial pCO_2 = 0.02 MPa; stirring rate = 300 rpm). A: pH, pCO_2 and EC. B: total uptake of CO_2, precipitated amount of carbonate, TDIC and dissolved contents of Ca and Mg per gram fly ash.

Al_2O_3 (2.7 ± 0.9) K_2O (0.4 ± 0), and C_{tot} (6.5 ± 0.5) as determined by XRF and CNS. After separating residual coal particles the content of organic carbon decreased to 2.5 wt.-% ± 0.5 wt.-%.

The untreated ash generally seems to be very fine-grained with more than 90% of the particles being smaller than 100 μm (cf. Supporting Information section D) containing a large surface area of 38 m^2 g^{-1}.

Reaction between Fly Ash and Water. The ANC of the fly ashes seems to be controlled by the dissolution of lime as indicated by the release of Ca with values up to 6 meq (g ash)$^{-1}$ at pH 7 after only 60 min of reaction at a s/l-ratio of 12.5 g L^{-1} (Figure 1A). The initial release rate of Ca increases with decreasing pH, i.e. with increasing distance from the solubility equilibrium of lime. Mg release became relevant only at pH < 8 with a maximal concentration of 0.4 meq g^{-1} at pH 7. Contrary to lime, dissolution of periclase as the Mg bearing phase requires neutral to acidic conditions to allow detachment of surface bound Mg^{2+} (*16*).

The absence of Fe and Al in solution coincides with the observed precipitation of ettringite ($Ca_6(Al(OH)_6)_2(SO_4)_3 \cdot 26H_2O$) of ~ 3 wt.-% (data not shown) and also reflects the low solubility of brownmillerite and gehlenite.

Once exposed to water, the fly ashes were highly soluble and showed a rapid release of the main constituents Ca, Na, SO_4^{2-} and OH^- into the solution (Figure 1B), which was accompanied by a strong increase of pH (up to 12.8) and electric conductivity (EC) up to 11 mS cm^{-1} only seconds after addition of the ashes.

Na concentrations released from fly ashes remained almost unchanged over the whole experimental run, suggesting that the dissolution of Na_2SO_4 was complete already after the first minutes (eq 2):

$$Na_2SO_4(s) \rightarrow 2Na^{2+}(aq) + SO_4^{2-}(aq) \quad (3)$$

The amount of sulfate was nearly twice the value of Na indicating also the dissolution of anhydrite in the initial phase, the content of which decreased by 30% within the experimental period. Ca together with OH^- concentrations further increased with time. Ca release appears to occur in two stages: an initial rapid release due to the dissolution of both, anhydrite, (eq 3)

$$CaSO_4(s) \rightarrow Ca^{2+}(aq) + SO_4^{2-}(aq) \quad (4)$$

and of lime (eq 4):

$$CaO(s) + H_2O(l) \rightarrow Ca^{2+}(aq) + 2OH^-(aq) \quad (5)$$

which explains also the rapid increase of the pH. Similar to the observations made at constant pH (Figure 1B), the dissolution rate of lime seems to decelerate upon increase of the pH which we attribute to both, the saturation with respect to lime and the exhaustion of the lime pool (11.5 to ~3 wt.-% after 10 min, Table 1).

Reaction between CO_2 and Fly Ash. Figure 2A shows the temporal variation of pH, EC and pCO_2 during one experimental run. Three reaction phases can be identified that can be separated according to the two 2 pH-inflection points i_1 at pH 10.3 and i_2 at pH 8.3.

Phase I is characterized by high pH values accompanied by a strong increase of EC. The inflection point matches the equivalence point of the CO_3^{2-}/OH^--system which, depending on the TDIC concentration, is located at pH ≈ 10.3 (*17*). Hence, the high pH values measured in phase I reflect the caustic alkalinity generated by the dissolution of lime (eq 4). Dissolution of periclase

$$MgO(s) + H_2O(l) \rightarrow Mg^{2+}(aq) + 2OH^-(aq) \quad (6)$$

is negligible in this phase since its dissolution rate is low at high pH (*16*).

The occurrence of caustic alkalinity suggests that the dissolution of lime is significantly faster in this phase than the OH^--consuming carbonation reaction. This assumption is supported by the build-up of high Ca concentrations after only seconds of reaction. The following drop of EC, accompanied by a decrease of Ca in solution, denotes the onset of the carbonation reaction (eq 6) after 5 min,

$$Ca^{2+}(aq) + HCO_3(aq) \xrightarrow{k_{carb}} CaCO_3\downarrow(s) + H^+(aq) \quad (7)$$

which is accompanied by a maximum CO_2 uptake of 0.7 mmol g^{-1} after 10 min (the 2−3 min delay of the pCO_2 minimum relative to the EC maximum is caused by the inertia of the CO_2-sensor). Rapid calcite precipitation in phase I could be confirmed by XRD measurements. Calcite seems to be the only carbonate mineral since magnesium carbonates were not detectable in the CO_2-treated fly ash samples at any time. The continuous drop in pH therefore seems to be related to the direct transfer of Ca from the lime pool into calcite. Exhaustion of this pool decreases the dissolution rate of lime to values significantly lower than the carbonation rate which then leads to a significant shift of the pH regime into the carbonate buffer system.

Carbonation seems to be fast relative to the transfer of gaseous CO_2 into the aqueous phase since no build-up of TDIC in this initial phase was observed. At the present high pH values however (>9) the CO_2 transfer is predominated by the reaction path desribed in eq 8. The forward rate constant k_{CO2} given in literature is 8.5×10^{-3} L mol^{-1} s^{-1} (*17*), resulting in higher rates than observed in our study at pH 12 (0.026 mmol L^{-1} s^{-1}):

$$CO_2 + OH^- \xrightarrow{k_{CO_2}} HCO_3 \xrightarrow{\text{very fast}} CO_3^{2-} + H^+ \quad (8)$$

Phase II is dominated by the carbonation reaction that

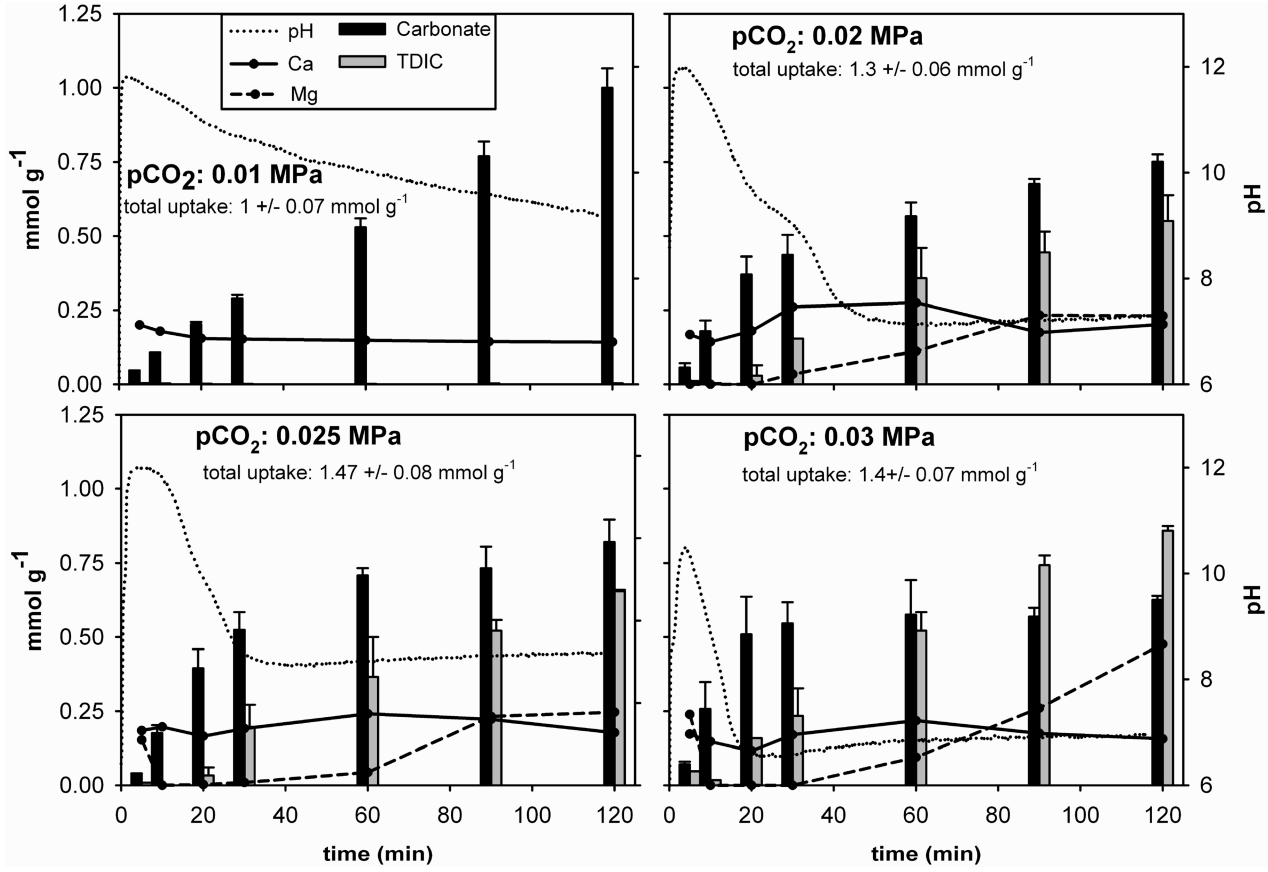

FIGURE 3. CO_2-transfer (millimoles per gram fly ash) into carbonate and TDIC as a function of pCO_2 (s/l = 75 g L^{-1}; T = 25 °C; stirring rate = 450 rpm; gas flux = 1 L min^{-1}). Experimental accuracy was calculated based on replication of experiments at least twice.

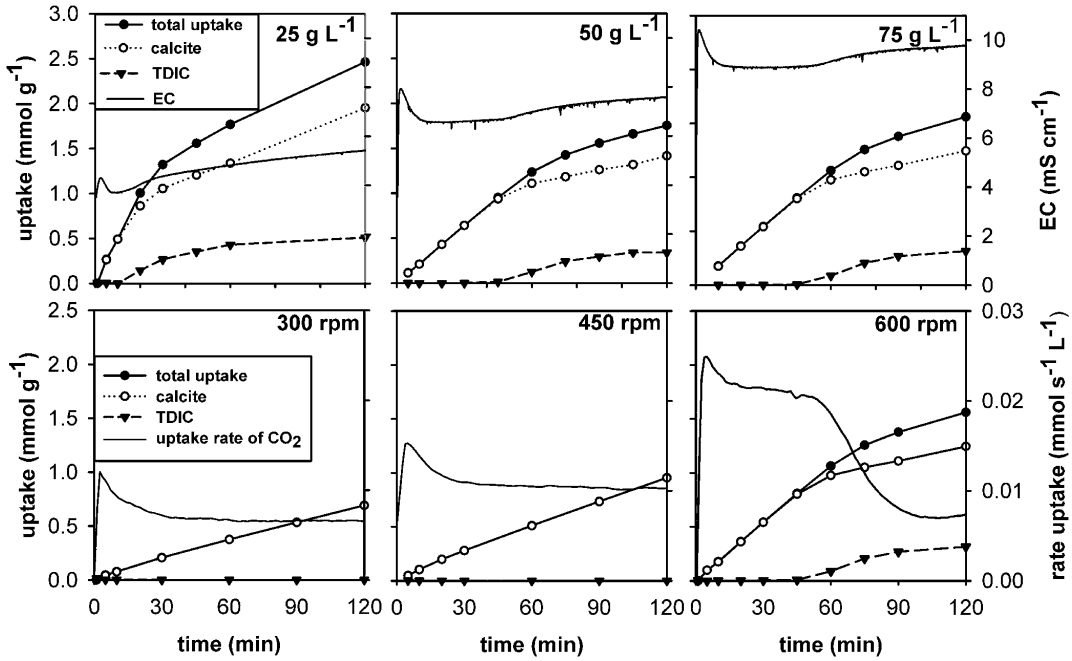

FIGURE 4. Dependence of CO_2 transfer at 25 °C and pCO_2 = 0.01 MPa on top: s/l-ratio (stirring rate 600 rpm) and bottom: stirring rate (s/l-ratio 75 g L^{-1}).

consumes alkalinity and drives the pH toward lower values. The onset of HCO_3^- formation (as TDIC) at the end of phase II indicates deceleration of the carbonation reaction which is due to exhaustion of the lime pool. The pH of the solution is now buffered by the equilibrium between dissolved CO_3^{2-} and HCO_3^- so that the pH rapidly decreases to values below the equivalence point of this buffering system (pH 8.3).

CO_2 uptake in phase III is to a significant extent controlled by the formation of TDIC. Only now, also periclase dissolves

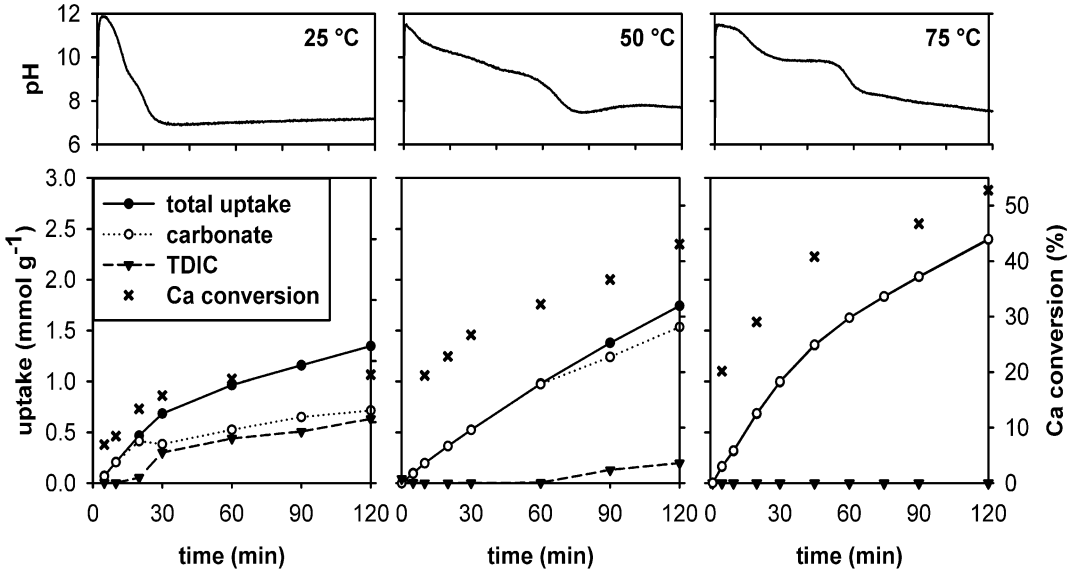

FIGURE 5. Dependence of CO_2 transfer on temperature (pCO_2 = 0.02 MPa, stirring rate 600 rpm, s/l-ratio 75 g L^{-1}). Top: time course of pH, bottom: CO_2 transfer. Note that the total uptake of CO_2 at 75 °C is identical to the amount of carbonate precipitated.

(eq 5) which neutralizes CO_2 mainly as dissolved Mg-bicarbonate.

The pH remains nearly unchanged during this phase suggesting that proton consumption in reaction 5 and proton generation in reaction 7 balance each other under these conditions. The coupled increase of TDIC and Mg^{2+} at the end of the experiments implies that dissolution of periclase controls the CO_2 transfer during this phase. Mg concentrations are almost balanced by the generation of TDIC.

To summarize, the time response of the reaction between CO_2 and fly ashes in aqueous solutions is mainly driven by the rates of alkalinity providing reactions, i.e., dissolution of lime and periclase, and rates of alkalinity consuming reactions, i.e., precipitation of calcite and build-up of TDIC. These reactions control the pH which itself feeds back on the reaction velocities of the individual reactions and on the pathways of the reaction. In the following we will discuss the effect of the process variables on the development of the various process phases and how they control the CO_2 uptake.

Effect of Process Variables on CO_2 Uptake. *CO_2 Partial Pressure.* The effect of the pCO_2 on the CO_2 uptake was tested at pCO_2 = 0.01, 0.02, 0.025, and 0.03 MPa. At the lowest pCO_2 the pH never fell below 9 (Figure 3). Neither TDIC nor Mg^{2+} could be detected which implies that CO_2 is completely transformed into calcite. At higher pCO_2 values a significant drop of the pH can be observed after 10−20 min accompanied by a build-up of Mg^{2+} and TDIC. Calcite still precipitated once phase III (pH < 8.3) had established, although at a significantly lower rate. The total uptake of CO_2 under these conditions was increased from 1.0 mmol g^{-1} (pCO_2 = 0.01 MPa) to 1.47 mmol g^{-1} (pCO_2 = 0.025 MPa) due to the coeval precipitation of carbonate and formation of TDIC.

At the highest pCO_2 applied in the experiments (pCO_2 = 0.03 MPa) the lowest pH values were measured. Calcite precipitation finished after only 20 min at a pH of approximately 6.6, reducing the net uptake of CO_2 to 1.4 mmol g^{-1} after 120 min of reaction even though higher TDIC values were observed..

It appears that the supply rate of alkalinity from dissolution of lime is not sufficient to maintain a pH high enough for calcite precipitation at high pCO_2 values, which is due to an increased dissolution rate of CO_2 at higher partial pressure. pH-stat experiments performed in deionized water (pH 9, T = 25 °C, stirring rate: 300 rpm) demonstrated that the dissolution rate of CO_2 increased almost linear from 0.007 mmol L^{-1} at a pCO_2 of 0.01 MPa to 0.02 mmol L^{-1} at a pCO_2 of 0.03 MPa.

To summarize, the effect of pCO_2 on CO_2 uptake is 2-fold. Higher pCO_2 values lead to a temporal shift of the pH regime that significantly affects the pathways of CO_2 uptake. The uptake rate is generally enhanced at higher pCO_2 due to the higher dissolution rate of CO_2. Above a threshold of pCO_2 = 0.025 MPa a pH establishes (<6.9) that suppresses calcite formation during phase II and thus reduces the amount of CO_2 sequestered.

Solid−Liquid-Ratio. Variation of the s/l-ratio strongly affects the pH by the amount of OH^- ions released from the alkaline mineral compounds. The more fly ash is available, the longer lasts phase I, as indicated by the minimum of EC (Figure 4 top).

At the lowest s/l-ratio (25 g L^{-1}, pCO_2: 0.01 MPa, Figure 4 top) the highest degree of calcite precipitation was observed with 2.5 mmol CO_2 neutralized per g fly ash and nearly 40% of the total Ca released from the fly ash compounds, even though calcite precipitation was not yet finished.

Lower s/l-ratios seem to generally increase the Ca release rate and the rate of the CO_2 uptake due to a dilution effect. The larger the volume of water the larger is the solubility of the Ca and Mg bearing mineral phase and the capacity to dissolve CO_2. On the other hand, absolute uptake rates of CO_2 are increased with higher s/l-ratios due to a stronger pH buffer effect (data not shown) resulting in an enhanced dissolution rate of CO_2. The CO_2 uptake per gram fly ash and the time response of the system are therefore almost similar for 50 and 75 g L^{-1} of suspended ash.

Stirring Rate. The total uptake of CO_2 increased from 0.7 mmol g^{-1} at 300 rpm to 1.6 mmol g^{-1} at 600 rpm after 120 min with 23% of Ca converted mainly into calcite at this rate (Figure 4 bottom).

The rates of CO_2 uptake (mmol s^{-1} L^{-1}) remained constant during the whole experiment at the lower stirring rates (300 and 450 rpm) after a sharp increase in the first seconds. The constant uptake rates were accompanied by a linear increase of the amount of CO_2 sequestered as calcite. The system remained in phase I and II during the whole experimental time (pH > 9). At 600 rpm the reaction shifts from phase II to phase III after ~60 min as indicated by the onset of TDIC formation and reduced uptake rates of CO_2 due to reduced calcite formation.

CO_2 uptake rates measured during the period of carbonation in all experiments (0.007−0.021 mmol L^{-1} s^{-1}) correspond to the dissolution rates of CO_2 as determined during independent pH-stat experiments to test the effect of the stirring rate on CO_2 dissolution in water at pH 10. In these experiments, CO_2 dissolution rates were found to increase from 0.007 ± 0.001 mmol s^{-1} L^{-1} at 300 rpm to 0.019 ± 0.001 mmol s^{-1} L^{-1} at 600 rpm, which is due to the reduction of the size of the gas bubbles mixed into the aqueous phase by the stirring activity and a subsequent increase of their surface area. The match between CO_2 uptake rates and CO_2 dissolution rates implies that the latter process is the rate limiting step during phase I.

The high initial uptake rates of CO_2 seem to be limited by the transport of CO_2 to the mineral surface that can be enhanced with increasing stirring rate (*18*).

Temperature. Figure 5 illustrates the effect of a temperature increase from 25 to 75 °C on the CO_2 uptake. The higher the temperature, the longer the pH remains buffered by caustic alkalinity, which we interpret to be due to two effects: Raising the temperature on the one hand increases the dissolution rate of the basic mineral compounds (*16*) and on the other hand decreases the solubility of CO_2 in water (*17*). The increase of the CO_2 uptake with temperature can, therefore, mainly be attributed to the rising formation of carbonate and extension of phase I and phase II (see pH, Figure 5). At 75 °C, mainly calcite precipitation accounts for the uptake of CO_2 with more than 95% of the totally released Ca converted into calcite after 2 h of reaction.

The rate of calcite precipitation at 75 °C has nearly doubled (∼0.05 mmol s^{-1} L^{-1}) compared to values observed at 25 °C (∼ 0.03 mmol s^{-1} L^{-1}). More than 50% of the total Ca content of the fly ashes had been converted into calcite after 120 min. Rising concentrations of dissolved Al (maximal 10 mmol L^{-1}) at 75 °C are observed and indicate the onset of the dissolution of less soluble Ca compounds (in particular brownmillerite) contributing to the increased Ca-conversion. Thus, enhanced carbonation is mainly due two factors: (i) the enhanced release of Ca from the mineral compounds at higher temperature and (ii) the increased rate of calcite precipitation at higher temperature (*19*).

In order to determine the maximum CO_2 sequestration potential at 75 °C, experiments were conducted until the pCO_2 at the outflow reached the value at the inflow of the reactor (data not shown). After 270 min of reaction (s/l-ratio: 50 g L^{-1}, pCO_2: 0.01 MPa, stirring rate: 600 rpm), an uptake of 5.2 mol CO_2 per kg fly ash (∼ 0.23 kg CO_2 per kg fly ash) was achieved. More than 75% of the available Ca was converted into calcite, 90% of the total uptake could be related to the precipitation of calcite, and almost 90% of the neutralizing capacity determined as ANC (6 meq g^{-1}) was consumed by the reaction with CO_2.

Implications for a Technical Realization. The maximum conversion of 5.2 moles of CO_2 per kg fly ash (≈ 0.23 kg kg^{-1}) obtained at 75 °C demonstrates the potential of alkaline fly ashes to sequester CO_2. This value accounts for a CO_2 sequestration capacity of nearly 3.5 million t of CO_2 in Germany alone based on the available lignite fly ash, which corresponds to 2% of the CO_2 emissions from lignite power combustion (175 million t a^{-1} (*20*)).

Our results have outlined the geochemical framework for the technical use not only of lignite ashes for CO_2 sequestration but also of alkaline combustion residues in general. Although the process chain has been elucidated for low s/l-ratios only, it is reasonable to assume that the general principles can be also used at higher ratios, e.g., the so-called semidry process route (Baciocchi et al., 2006). In order to provide a rapid uptake at a time scale of minutes, it is necessary to keep the reaction in phase I with the highest CO_2-uptake rates. Establishing a balance between alkalinity providing and consuming reactions is therefore a prerequisite to achieve the adequate pH values, which can be best obtained at enhanced temperature and by maximizing the dissolution rate of CO_2. Contrary to our experimental systems, where CO_2 dissolution was rate limiting, this process can be significantly accelerated in technical systems which will minimize the residence time in a reactor plant.

It appears that the maximum rates of carbonation and formation of dissolved Mg-bicarbonate occur at different pH values. This pool could be made available for mineral trapping if the kinetic restrictions for precipitation of Mg-carbonate can be overcome, e. g. by running the processes at higher temperature (>50 °C) and higher s/l-ratio (*21*).

Acknowledgments

We thank M. Heider and D. Kuenkel for technical assistance and M. Bauer for valuable discussions. M. Back was supported by the German Ministry of Education and Research (BMBF, Grant 03G0614A).

Supporting Information Available

The experimental setup, details on the used methods to determine the CO_2-transfer, SEM pictures taken from the lignite fly ashes, grain size analysis, and mineralogical composition calculated by Rietveld analysis. This material is available free of charge via the Internet at http://pubs.acs.org.

Literature Cited

(1) Lackner, K. S.; Wendt, C. H.; Butt, D. P.; Joyce, E. L.; Sharp, D. H. Carbon dioxide disposal in carbonate minerals. *Energy* **1995**, *20*, 1153–1170.

(2) Wolff-Boenisch, D.; Gislason, S. R.; Oelkers, E. H. The effect of crystallinity on dissolution rates and CO_2consumption capacity of silicates. *Geochim. Cosmochim. Acta* **2006**, *70*, 858–870.

(3) Huijgen, W. J. J.; Witkamp, G. J.; Comans, R. N. J. Mechanisms of aqueous wollastonite carbonation as a possible CO_2 sequestration process. *Chem. Eng. Sci.* **2006**, *61*, 4242–4251.

(4) Teir, S.; Eloneva, S.; Zevenhoven, R. Production of precipitated calcium carbonate from calcium silicates and carbon dioxide. *Energy Convers. Manage.* **2005**, *46*, 2954–2979.

(5) Huijgen, W. J. J.; Ruijg, G. J.; Comans, R. N. J.; Witkamp, G. J. Energy consumption and net CO_2 sequestration of aqueous mineral carbonation. *Ind. Eng. Chem. Res.* **2006**, *45*, 9184–9194.

(6) Huijgen, W. J. J.; Witkamp, G. J.; Comans, R. N. J. Mineral CO_2 sequestration by steel slag carbonation. *Environ. Sci. Technol.* **2005**, *39*, 9676–9682.

(7) Soong, Y.; Fauth, D. L.; Howard, B. H.; Josnes, J. R.; Harrison, D. K.; Goodman, A. L.; Gray, M. L.; Frommell, E. A. CO_2sequestration with brine solution and fly ashes. *Energy Convers. Manage.* **2006**, *47*, 1676–1685.

(8) Stolaroff, J. K.; Lowry, G. V.; Keith, D. W. Using CaO- and MgO-rich industrial waste streams for carbon sequestration. *Energy Convers. Manage.* **2005**, *46*, 687–699.

(9) RWE. *Handbuch der Verwertung von Braunkohlenfilteraschen in Deutschland*; RWE-Aktiengesellschaft, Zentralbereich Forschung und Entwicklung: Essen, 1995.

(10) Fernandez Bertos, M.; Simons, S. J. R.; Hills, C. D.; Carey, P. J. A. review of accelerated carbonation technology in the treatment of cement-based materials and sequestration of CO_2. *J. Hazard. Mater.* **2004**, *112*, 193–205.

(11) Meima, J. A.; van der Weijden, R. D.; Eighmy, T. T.; Comans, R. N. J. Carbonation processes in municipal solid waste incinerator bottom ash and their effect on the leaching of copper and molybdenum. *Appl. Geochem.* **2002**, *17*, 1503–1513.

(12) Querol, X.; Umana, J. C.; Alastuey, A.; Ayora, C.; Lopez-Soler, A.; Plana, F. Extraction of soluble major and trace elements from fly ash in open and closed leaching systems. *Fuel* **2001**, *80*, 801–813.

(13) Commission Decision 2000/532/EC2. Official Journal of the European Communities. 2000, L226/3.

(14) Bertos, M. F.; Li, X.; Simons, S. J. R.; Hills, C. D.; Carey, P. J. Investigation of accelerated carbonation for the stabilisation of MSW incinerator ashes and the sequestration of CO_2. *Green Chem.* **2004**, *6*, 428–436.

(15) Bergmann, J.; Kleeberg, R. Rietveld analysis of disordered layer silicates In *Epdic 5*, Pts 1 and 2, 1998; *278*−*2*, 300305.
(16) Vermilye, D. A. Dissolution of MgO and $Mg(OH)_2$ in aqueous solutions. *J. Electrochem. Soc.* **1969**, *116*, 1179–1183.
(17) Stumm, W.; Morgan, J. J. *Aquatic Chemistry*, 3rd ed.; John Wiley & Sons, Inc.: New York, 1996.
(18) Liu, Z. H.; Dreybrodt, W. Dissolution kinetics of calcium carbonate minerals in H_2O-CO_2 solutions in turbulent flow: The role of the diffusion boundary layer and the slow reaction $H_2O + CO_{2>} \leftarrow H^+ + HCO_3$. *Geochim Cosmochim. Acta* **1997**, *61*, 2879–2889.
(19) Buhmann, D.; Dreybrodt, W. The kinetics of calcite dissolution and precipitation in geologically relevant situations of karst areas 0.1. open system. *Chem. Geol.* **1985**, *48*, 189–211.
(20) DIW. *Innovative Energy Technologies and Climate Policy in Germany*; German Institute for Economic Research, 2005.
(21) Hänchen, M.; Prigiobbe, V.; Baciocchi, R.; Mazotti, M. Precipitation in the Mg-carbonate system-effects of temperature and CO_2 pressure. *Chem. Eng. Sci.* **2008**, *63*, 1012–1028.

ES702760V